18-years of high-Alpine rock wall monitoring using terrestrial laser scanning at the Tour Ronde east face, Mont-Blanc massif

Léa Courtial-Manent, Ludovic Ravanel, Jean-Louis Mugnier, Philip Deline, Alexandre Lhosmot, Antoine Rabatel, Pierre-Allain Duvillard, Philippe Batoux

ENVIRONMENTAL RESEARCH
LETTERS

LETTER • OPEN ACCESS

18-years of high-Alpine rock wall monitoring using terrestrial laser scanning at the Tour Ronde east face, Mont-Blanc massif

ENVIRONMENTAL RESEARCH
LETTERS

OPEN ACCESS

RECEIVED
16 October 2023

REVISED
13 December 2023

ACCEPTED FOR PUBLICATION
9 February 2024

PUBLISHED
27 February 2024

LETTER

18-years of high-Alpine rock wall monitoring using terrestrial laser scanning at the Tour Ronde east face, Mont-Blanc massif

Léa Courtial-Manent[1,2,*], Ludovic Ravanel[2], Jean-Louis Mugnier[1], Philip Deline[2], Alexandre Lhosmot[3], Antoine Rabatel[4], Pierre-Allain Duvillard[5] and Philippe Batoux[6]

[1] ISTerre, Université Grenoble Alpes, University Savoie Mont Blanc, CNRS, IRD, University G. Eiffel, 38000 Grenoble, France
[2] EDYTEM, Université Savoie Mont-Blanc, CNRS (UMR 5204), 73370 Le Bourget du Lac, France
[3] Chrono-Environnement, Université de Franche-Comté, CNRS (UMR 6249), Besançon, Montbéliard, France
[4] Université Grenoble Alpes, CNRS, IRD, Grenoble INP, IGE, 38400 Grenoble, France
[5] Nāga Geophysics, Technolac, 73370 Le Bourget-du-Lac, France
[6] ENSA, ENSM, 74400 Chamonix, France
[*] Author to whom any correspondence should be addressed.

E-mail: lea.courtial-manent@univ-smb.fr

Keywords: rockfalls, erosion rates, permafrost degradation, glacier retreat, terrestrial laser scanning, Mont-Blanc massif

Supplementary material for this article is available online

Abstract

Since the end of the 20th century, each decade has been warmer than the previous one in the European Alps. As a consequence, Alpine rock walls are generally facing high rockfall activity, likely due to permafrost degradation. We use a unique terrestrial laser scanning derived rockfall catalog over 18 years (2005–2022) compared with photographs (1859–2022) to quantify the evolution of the east face of Tour Ronde (3440–3792 m a.s.l.) in the Mont-Blanc massif (western European Alps) that is permafrost-affected. Overall, 210 rockfalls were identified, from 1 to 15 500 m^3. Forty-five events were >100 m^3 while cumulated volume of events <10 m^3 represents <1% of the fallen rocks. The rockfall magnitude-frequency distribution of the overall inventory follows a power law, with a mean exponent b of 0.44 ± 0.03, characterizing a high contribution of large rockfalls. The depth of failure ranges from a few centimeters to more than 20 m while 95% of the rockfalls depth is <5 m, highlighting the role of the active layer. The mean rock wall erosion rate is 18.3 ± 0.2 mm yr^{-1} for the 2005–2022 period and ranks in the top range of reported values in the Alps. It has greatly increased between the periods 2006–2014 and 2016–2022, probably in relation to a series of summer heat waves. The exceptional erosion rate of 2015 is driven by one large rockfall in August. Since 2006, an ice apron that covered 16 100 m^2 has now almost vanished, and the surface of the glacier du Géant at the rock wall foot has lowered by several tens of meters. The retreat of these two ice masses contributed to the rock wall instability as more than 35% of the rockfall volume detached from the deglaciated surfaces.

1. Introduction

Over the past three decades, a significant number of rockfalls from high Alpine rock walls located in permafrost-prone areas (Noetzli *et al* 2003, Legay *et al* 2021) globally have been studied (Haeberli *et al* 2004, Huggel *et al* 2005, Lipovsky *et al* 2008, Frauenfelder *et al* 2018). In the European Alps, studies focused on high-magnitude events like rock/ice avalanches, with volumes exceeding 2 × 10^6 m^3 (Deline 2001, Pirulli 2009, Deline *et al* 2015, Phillips *et al* 2017, Mergili *et al* 2020, Walter *et al* 2020). Smaller rockfalls have also been studied, such as at the Aiguilles Marbrées (Mont-Blanc massif, MBM hereafter; Curtaz *et al* 2014).

A clear correlation between periods of high temperature and rockfalls has been shown in the European Alps (Huggel *et al* 2012, Stoffel and Huggel 2012). Schiermeier (2003) showed that normally frozen landscapes were destabilized because ice was

thawing below 4500 m a.s.l. (all elevations are in m above sea level). In the MBM, this correlation has been demonstrated since the end of the Little Ice Age at the west face of the Petit Dru (3754 m) and on the north side of the Aiguilles de Chamonix (2300–3842 m; Ravanel and Deline 2008, 2011). More recently, Ravanel *et al* (2017) showed the impact of the 2003 and 2015 summer heatwaves on permafrost-affected rock walls in the MBM. In high Alpine areas, permafrost degradation (*i.e.* warming) due to global warming (Magnin *et al* 2017, Biskaborn *et al* 2019) is increasingly considered as a major factor for rock wall destabilization (Gruber *et al* 2004, Gruber and Haeberli 2007, Krautblatter *et al* 2013). This is in relation to a deepening of the active layer (the layer above the permafrost, subject to annual freeze/thaw cycles).

Other potential factors such as seismic activity (Keefer 2002, Jibson *et al* 2006, Kargel *et al* 2016), rock structure and lithology (McColl 2012), rock wall slope angle, hydrostatic pressure (Gruber *et al* 2004, Gruber and Haeberli 2007, Draebing *et al* 2014), thermal stress (Hall 1999, Matsuoka and Murton 2008, Huggel 2009, Gischig *et al* 2011, Draebing and Krautblatter 2019, Legay *et al* 2021), and paraglacial rock slope readjustment also contribute to destabilize rock walls (Ballantyne 2002, Cossart *et al* 2008, Grämiger *et al* 2017, 2018).

Rockfalls are a threat for alpinists (Soulé *et al* 2014, Mourey *et al* 2018), with mountain infrastructures subject to deterioration related to permafrost degradation (Duvillard *et al* 2019). The ongoing effects of global warming are likely to exacerbate these issues (Chiarle *et al* 2021), making long-term rockfall monitoring necessary for effective risk assessment and mitigation (Bommer *et al* 2010, Duvillard *et al* 2021).

Rockfall monitoring helps in both understanding steep slopes response to climatic change and quantifying rockfall volume and rock wall erosion rate. Many studies used terrestrial laser scanning (TLS hereafter) to quantify rock wall erosion rates. However, the duration of these studies is generally less than 10 years (Rabatel *et al* 2008, Ravanel *et al* 2011, Kenner *et al* 2011, Hartmeyer *et al* 2020a, 2020b, Guerin *et al* 2020, Draebing *et al* 2022). Long-term monitoring of permafrost-affected rock walls is necessary to assess frequency, as well as volume and triggering factors, of rockfalls.

This article aims to address this need using a rockfall catalog from TLS campaigns over 18 years (2005–2022) on a particularly active rock wall of the MBM, the Tour Ronde east face (TREF hereafter, 3792 m). Some preliminary results were analyzed by Rabatel *et al* (2008) and Ravanel *et al* (2011) we present here the whole set of data, and analyze the distribution of the rockfall magnitude and thickness, their spatial distribution and the relation with the glacier retreat. Finally, the role of active layer thickening and paraglacial processes are discussed.

2. Study area

2.1. Geographical and geological context

The MBM extends over 550 km^2 in the western European Alps, with approximately 30% covered by glaciers (figure 1, Gardent *et al* 2014). Permafrost covers 45% of the 86 km^2 of rock walls steeper than 40° on the French side of the massif (Magnin *et al* 2015a). Air temperature rose by +2 °C at Chamonix (1042 m) between 1980 and 2020.

The MBM is formed of a complex metamorphic basement intruded by the large (∼225 km^2) and homogeneous Mont-Blanc granite pluton (Bussy and von Raumer 1994). This granite is affected by subvertical faults, shear zones of which two main clusters are oriented ∼N40 and N70 (Rossi 2005, Matasci *et al* 2018). These faults determine the distribution of granite peaks and couloirs (Bertini *et al* 1985). Seismic activity in the MBM is far from negligible with around forty events between 2005 and 2022 ranging in the magnitude between 2 and 4.9 (Cara *et al* 2007). Several rock avalanches occurred over the past centuries (Deline 2001, Deline and Kirkbride 2009). Since the 2000s, the MBM has been increasingly affected by numerous small-scale rockfall events (Ravanel *et al* 2010, Deline *et al* 2012). TREF was one of the most active rock walls in the MBM during the period 2005–2009 (Ravanel *et al* 2011).

TREF is a rock wall of approximately 82 000 m^2 between 3440 and 3792 m, in the central part of the MBM, close to the Italian border (figure 1). Two major faults oriented N68E, passing by the Freshfield Pass and at the footwall of the Bernezat Spur, define three distinct areas from a fracturing point of view (figure 2(a)). To the South of the Freshfield Pass, fracturing is almost vertical and very dense. To the North, the Bernezat Spur is formed of a rather compact rock. The center of the rock wall can be divided in two parts: the upper part and lower part. The upper part, formerly covered by an ice apron (IA hereafter, figure 2(b)), defined as small ice bodies lying on slopes >40° (Guillet and Ravanel 2020, Kaushik *et al* 2022, Ravanel *et al* 2023), depicts a complex pattern formed by a block chaos lying on a complex substratum. The lower part shows at least three fracture sets: one very steep with a N-trend, one parallel to the sub-vertical N70°E major faults, and one almost horizontal. TREF has a mean slope angle of 62°, varying from 45 to 85°.

More than 350 archive photographs of the TREF from the late 1850s onwards (figure 3) show the evolution of the Glacier du Géant and the IA on the top of TREF. Analysis of these photos shows a decreasing ice coverage and the continuous thinning of the Glacier du Géant since the mid-1980 (figure 2(b), Fischer *et al* 2015, Vincent *et al* 2017).

Tour Ronde was first climbed in 1867 and its normal route is a popular and relatively easy mountaineering route on the margin of the east

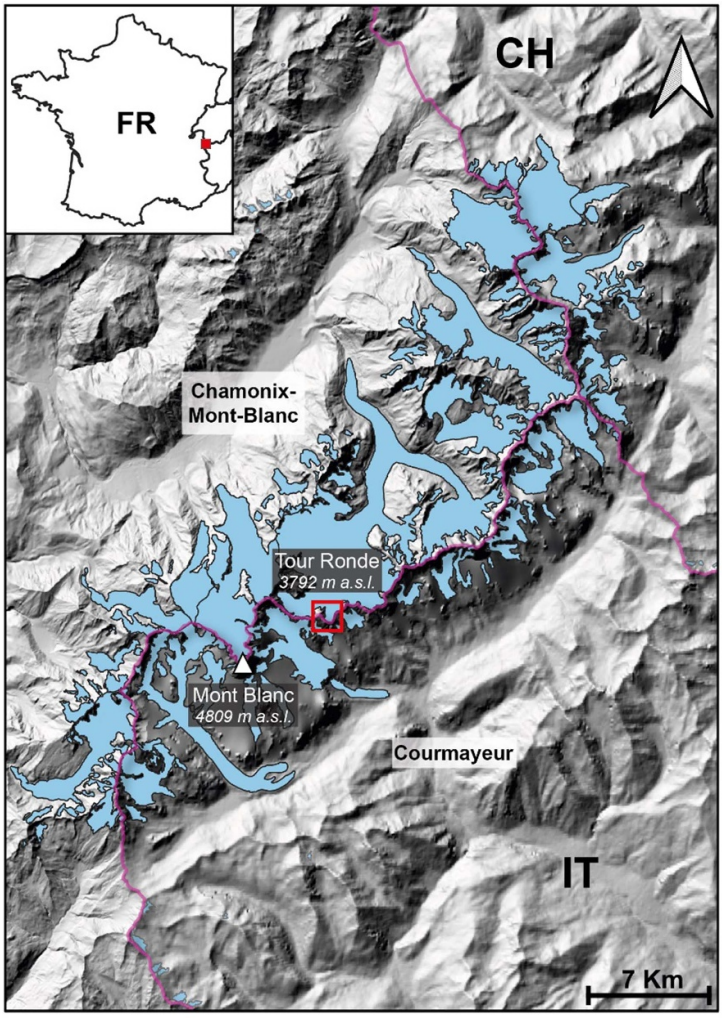

Figure 1. Mont-Blanc massif. Red square: location of the Tour Ronde east face (TREF, 3792 m a.s.l.); blue polygons: glaciers (Randolph Glacier Inventory (RGI) 2017).

face (figure 2(a)). In recent years the use of this route is declining in summer due to insufficient or no snow cover and hazardous conditions, making the Freshfield ridge a safer choice (Mourey *et al* 2019). The Bernezat spur was another well-known route.

2.2. Permafrost at TREF

Mean annual rock surface temperature (MARST) modeling of the whole face is around −2 °C (Magnin *et al* 2015a). Sub-surface thermistors recorded temperature at TREF between 2006 and 2009 (supplementary figure 1) and showed mean temperatures of −0.5 to −1.1, −0.7 to −1.3, and −1.1 to −1.7 °C, at depth of −3, −30, and −55 cm, respectively. Temperature ranges from −19 °C to +14 °C at the surface, and from −12 °C to +9 °C at −55 cm. Compared to Aiguille du Midi (3745 m, Magnin *et al* 2015b), TREF has a warmer permafrost thermal regime, with likely a thicker active layer which is at least 3 m thick. Furthermore, thermal modeling performed by Legay *et al* (2021) at the location of the largest rockfall of TREF (August 2015) indicates a temperature of 0 °C at a depth of around 8 m just before the collapse.

3. Methods

3.1. TLS data acquisition and processing

TLS technology is based on the acquisition of point clouds of topography using a time-of-flight distance measurement of an infrared laser pulse (see supplementary materials for details). It is a powerful method to monitor rock wall erosion (Rosser *et al* 2005, Oppikofer *et al* 2009, Ravanel *et al* 2014). Our TLS campaigns are most generally carried out at the end of the summer to ensure minimum snow cover on the rock walls, with data acquisition from the Glacier du Géant surface. Over the 18 year monitoring period (2005–2022), the TREF was scanned 16 times with an average acquisition of 10 000 000 points and an accuracy of 7 mm at a distance of 100 m.

The obtained individual point clouds were aligned using CloudCompare software (Girardeau-Montaut 2015) to get a full high-resolution 3D-model of the rock wall. The difference between the most

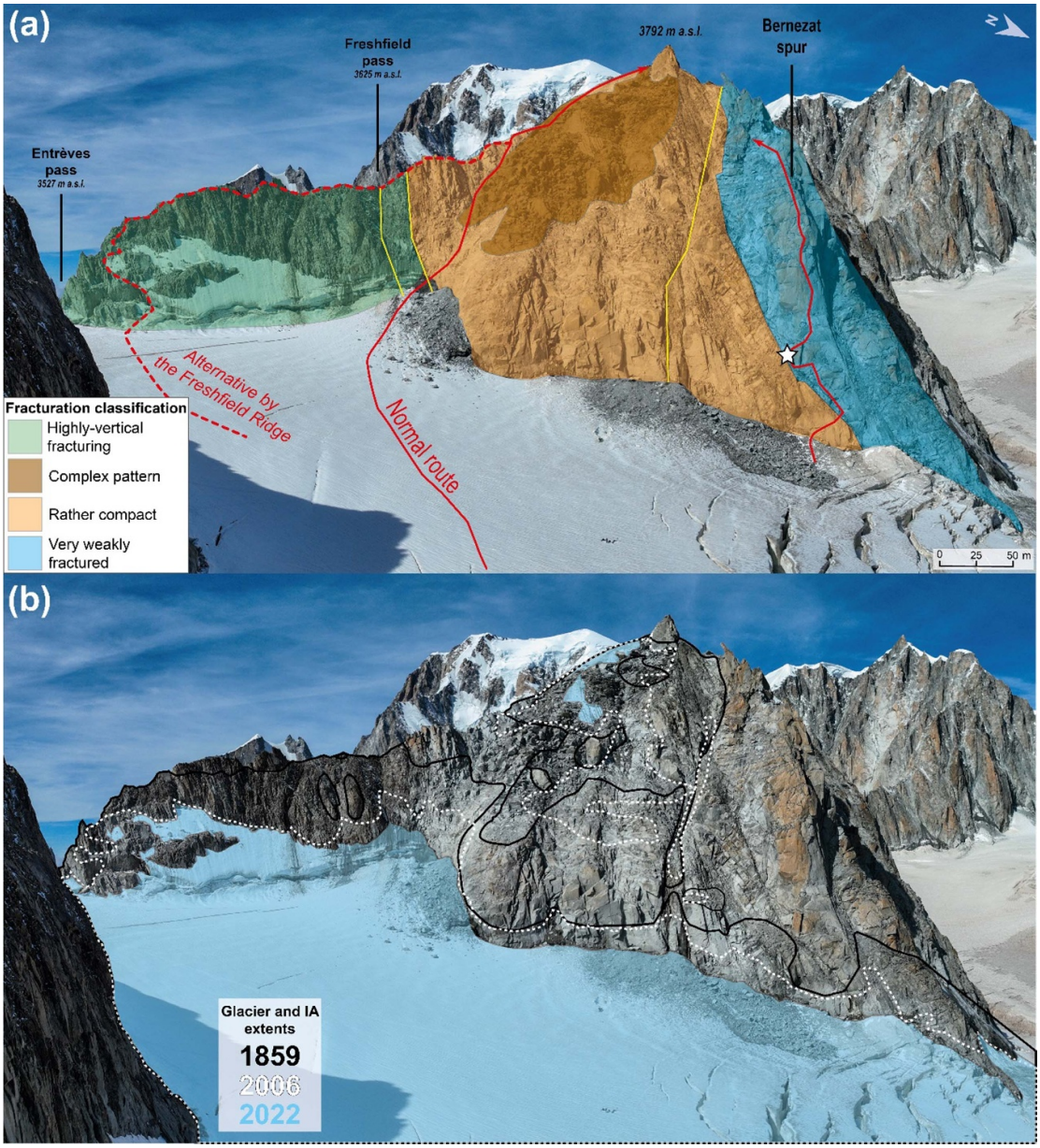

Figure 2. Tour Ronde east face in 2022. (a) Fracture types and distribution. Yellow: main faults; red: mountaineering routes; white star: location of the sub-surface thermistors; (b) shrinkage of the Glacier du Géant at the foot of the rock wall and of the ice apron (IA) on the upper part of TREF between 1859 and 2022.

recent acquisition and an older one allows morphological changes to be mapped (figure 4). Once differences resulting from changes in glacier, IA, and snow cover are removed, rockfalls are visually identified and their volumes computed using Poisson surface reconstruction algorithms (Kazhdan *et al* 2020). Every identified rockfall was measured using the software Cyclone 3DR (supplementary table 3; Leica Geosystems and Hexagon 2023). The erosion rate is the total volume lost between two successive field campaigns, divided by the smallest surface of acquisition of the rock wall (see supplementary materials for details).

Since only rockfalls with a minimum volume of several m^3 are relevant to study the potential effects of glacier retreat and permafrost degradation (Hartmeyer *et al* 2020a, 2020b, Graber and Santi 2022), rockfalls with volume <1 m^3 have been excluded.

3.2. Rockfall magnitude-frequency analysis

The frequency of rockfalls has a non-linear inverse relationship to its magnitude and follows a power law (equation (1); Dussauge *et al* 2003, Hantz *et al* 2003, Guerin *et al* 2020, Graber and Santi 2022):

$$F_p(V) = aV^{-b} \quad (1)$$

where $F_p(V)$ is the cumulative number of rockfalls in a given inventory, V the rockfall volume, p the period of interest, a the intercept and b the scaling exponent of the power law. The parameters a and b allow

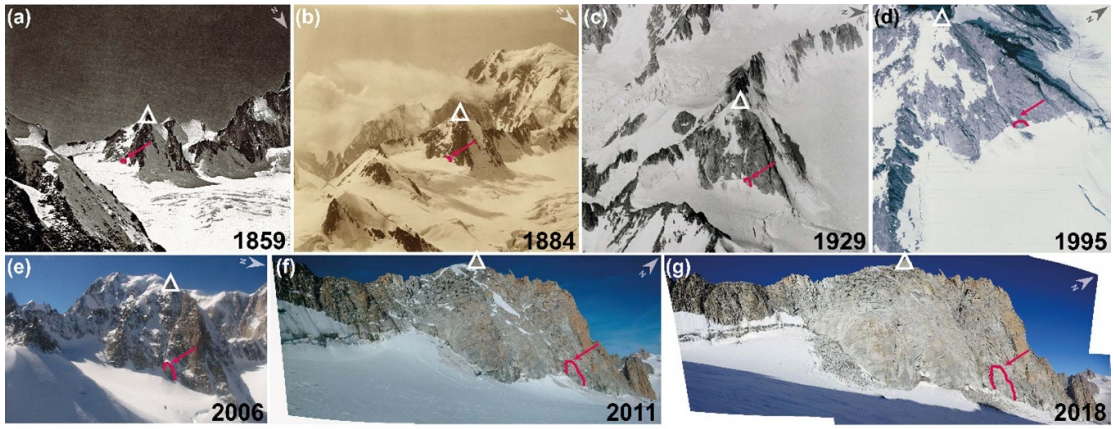

Figure 3. Archive photographs of TREF from the end of the little ice age (1859) to 2022. (a) Bisson brothers, Summer 1859 (detail); (b) V. Sella, Summer 1884 (detail); (c) W. Mittelholzer, Summer 1926; (d) IGN orthophoto, July 1995; (e) A. Rabatel, October 2006; (f) September 2011; (g) September 2018. These photographs particularly illustrate the evolution of Glacier du Géant located at the footwall of Tour Ronde. White triangle: summit (3792 m), red arrow: common point of reference, red polygons: pillar that collapsed on December 4th, 2018. The pillar culminates at 3510 m and the distance between TREF's summit and the pillar is 369 m.

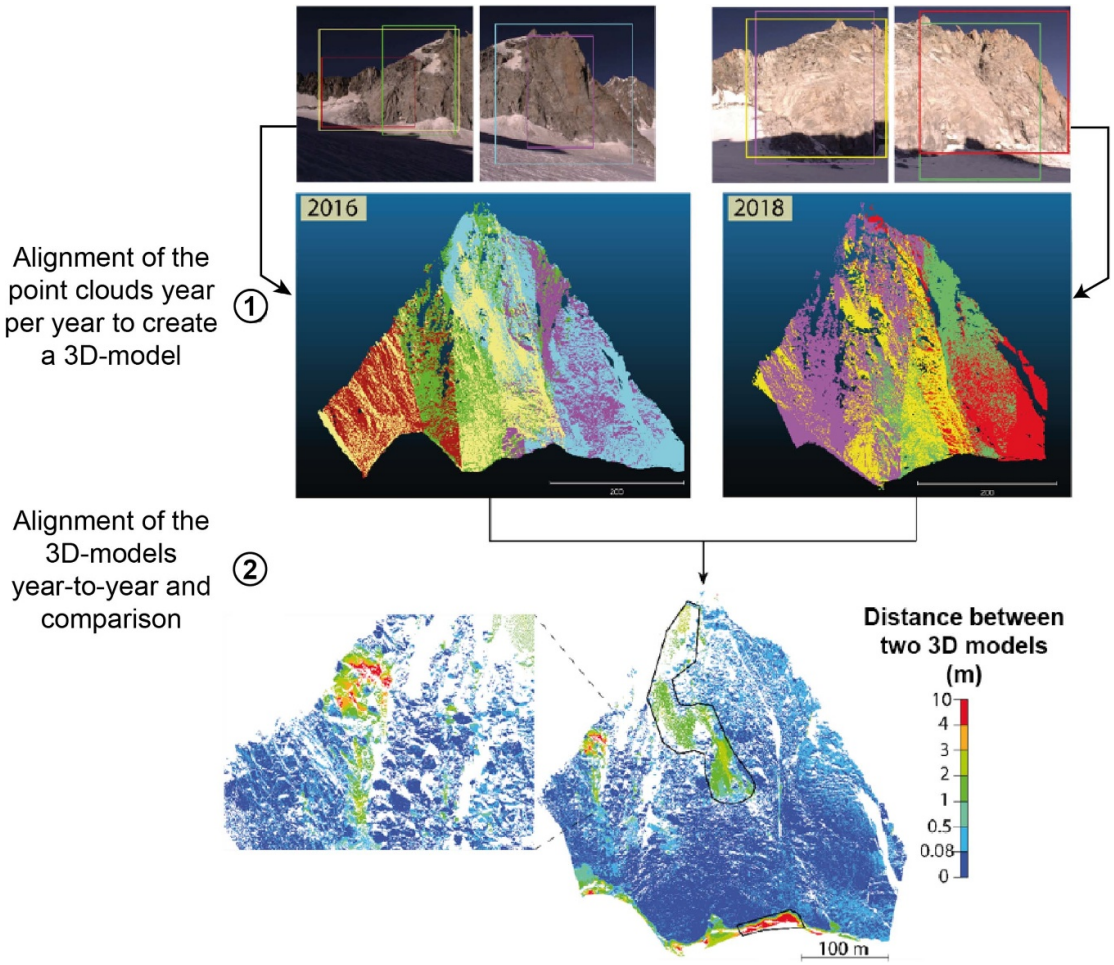

Figure 4. Workflow of the 3D point cloud comparison method for rockfall detection and volume estimation. Blue: small changes excluded from the interpretation. Green: changes related to glacier retreat (lower part of the face) or IA retreat (upper part). Red: major changes between two acquisitions with more than 10 m distance.

the comparison of different rockfall inventories from various locations or time periods (Graber and Santi 2022). The value of a gives the overall rockfall activity while the b-value gives information on the relative contribution of small rockfalls. Linear correlations r^2 of power laws and Δb uncertainty (Aki 1965) have also been calculated (see supplementary material, equation (3)).

4. Results

4.1. Rockfall inventory and magnitude-frequency relationship

On the 2005–2022 period, 210 rockfalls $\geqslant$1 m^3 were identified on the TREF. Rockfall volumes reach up to 15 578.3 $\pm$ 188 m^3 and the total rockfall volumes per year range from 71 $\pm$ 4 to 17 861 $\pm$ 204 m^3 (table 1). Rockfall volumes have a median of 10.3 m^3 and a mean of 248.9 m^3. Forty-five rockfalls (21%) are >100 m^3 and 104 (50%) <10 m^3. The total rockfall volume is 52 264.8 $\pm$ 631 m^3 corresponding to a mean erosion rate of 18.3 mm yr^{-1} (table 1).

2011–2015 is dominated by the 15 578 $\pm$ 188 m^3 rockfall. As this event occurred on 27th August 2015 (Ravanel *et al* 2017), the cumulated volume of 2011–2014 is therefore smaller than the difference between the cumulated 2011–2015 volume and the 2015 volume (table 2).

Mean detachment depths, inferred from the mean block thickness, range from 0.1 to 25 m (figure 5). 95% of the detachments are <5 m thick, 3% are between 5 and 10 m and 2% are >10 m. Over the entire period, the mean depth is 2.1 m and the median is 1.2 m. For the periods 2005–2008 (first period of acquisition) and 2021–2022 (last period of acquisition), with a total of 34 and 30 rockfalls respectively, the average maximum detachment depth is 1.5 m (median 1.0 m) and 2.1 m (median 1.8), respectively.

For the overall period (2005–2022), the rockfall magnitude-frequency distribution follows the power law function: $F_{2005\text{-}2022}(V) = 0.18\ V^{-0.44}$ (figure 6), with $b = 0.44 \pm 0.03$. The b-value evolution over time was studied for periods with at least 18 rockfalls, in order to reduce the Δb uncertainty to less than 0.1. Five single-year periods follow such a criterium and show a significant decrease, with values above-average in 2006 and 2009, and below-average in 2015, 2019 and 2022. When considering binning groups including all the data (class A, figure 7), the evolution is more complex, with in particular an increase in b for the period 2016–2018. This increase is not binning-dependent (see supplementary figure 2).

4.2. Description of the two main rockfalls at TREF

The largest rockfall occurred in August 2015 (www.youtube.com/watch?v=O2LL6fmKXck) on the left side of TREF, in a rather gentle slope area still covered by an IA in 1859 and characterized by a complex fracture pattern (figure 2(a)). Ravanel *et al* (2017) estimated its volume at 15 000 $\pm$ 3 000 m^3. Our study measured a volume of 15 578 $\pm$ 188 m^3 with an average thickness of 17 m. The MARST modeled there is between −1.6 °C (Legay *et al* 2021) and −2.3 °C (Ravanel *et al* 2017). According to Legay *et al* (2021), the temperature averaged over one day before the collapse was 10 °C at the surface and 0 °C at around 8 m depth. Massive ice and water flows were observed in the detachment scar.

A rockfall of 6791 $\pm$ 228 m^3 occurred on December 4th, 2018 in the lower part of the face (see supplementary material, figure 2). Tilting has been observed between September 2016 and September 2018. The collapsed pillar was 42 m high and 29 m wide, with a maximum thickness of 6 m. The scar corresponds to a large regular surface with a slope angle of 80°. Ice occupied the entire width of the scar with a thickness from a few tens of centimeters (bottom) to several meters (top; see supplementary material, figure 2(c)).

4.3. Rockfall locations compared to the retreat of Glacier du Géant and the IA, and the fracturing pattern

Photo-comparison (figure 2(b)) shows the lowering of the surface of the Glacier du Géant between 1859 and 2006, averaging 10 m between 2006 and 2022 (min: 0.9, max: 23.0 m; figure 8(a)). The surface area of the IA on the steep upper part of the face decreased by 68% (approximately 16 100 m^2 in 2006 and 5170 m^2 in 2022), hence dropping from 11%–3% of the total rock wall surface. Rockfall locations illustrated on figure 8 show that:

- Before 2018, only three rockfalls detached from areas deglaciated since 2006.
- During the 2018–2019 period, five and four rockfalls occurred, respectively, in the area uncovered by the IA and the Glacier du Géant since 2006, corresponding to 9% and 75% of the rockfall volume for this period.
- Between 2019 and 2021, three rockfalls occurred from the area uncovered by the IA, corresponding to 93% of the period volume, whereas no rockfall occurred in the Glacier du Géant deglaciated area.
- During the 2021–2022 period, six rockfalls (32% of the volume) were identified in the Glacier du Géant deglaciated area.
- 18 rockfalls out of 210 (around 10% of the total rockfall volume) affected the very weakly fractured area of the Bernezat Spur.

Table 1. Main characteristics of the rockfall inventory.

Scanning period	Rockfall number V >1 m^3	Maximum volume (m^3)	Total rockfall volume (m^3)	Erosion rate ($mm\ yr^{-1}$)
Jun 2005–Jul 2006 (1 yr)	13	490 ± 126	728 ± 128	10.2 ± 1.8
Jul 2006–Oct 2007 (1 yr)	14	566 ± 21	734 ± 48	7.0 ± 0.5
Oct 2007–Sep 2008 (1 yr)	7	179 ± 2	485 ± 253	4.6 ± 2.4
Sep 2008–Sep 2009 (1 yr)	22	262 ± 20	503 ± 277	4.4 ± 2.4
Sep 2009–Oct 2010 (1 yr)	6	20 ± 2	71 ± 4	0.7 ± 0.0
Oct 2010–Sep 2011 (1 yr)	3	134 ± 6	194 ± 7	2.0 ± 0.1
Sep 2011–Sep 2015 (4 yrs)	22	15 578 ± 188	17 861 ± 204	58.9 ± 0.7
Sep 2015–Sep 2016 (1 yr)	8	3 395 ± 167	5 961 ± 191	78.6 ± 2.5
Sep 2016–Sep 2018 (2 yrs)	57	4 173 ± 245	5 062 ± 246	21.7 ± 1.1
Sep 2018–Sep 2019 (1 yr)	20	6 791 ± 228	9 393 ± 573	80.6 ± 4.9
Sep 2019–Sep 2021 (2 yrs)	8	2 528 ± 265	3 835 ± 488	12.3 ± 1.6
Sep 2021–Aug 2022 (1 yr)	30	2 658 ± 119	7 439 ± 755	47.6 ± 4.8
Jun 2005–Aug 2022 (18 yrs)	**210**	**15 578 ± 188**	**52 265 ± 631**	**18.3 ± 0.2**

Table 2. Estimate (E) of the distribution of the rockfall volume during the 2011–2015 period, inferred from the cumulated volume between 2011 and 2015 and the occurrence of the large rockfall of 27th August 2015.

Type	Period	Maximum volume (m^3)	Total rockfall volume (m^3)	Erosion rate ($mm\ yr^{-1}$)
Scan acquisition	Sep 2011—Sep 2015 (4 years)	15 578 ± 188	17 861 ± 204	58.9 ± 2.1
Estimate (E)	Sep 2011–2014 (3 years)	?	$0 < E < 2\,282 \pm 392$	$0 < E < 10 \pm 1.7$
	2014–Sep 2015 (1 year)	15 578 ± 188	$15\,578 \pm 188 < E < 17\,861 \pm 204$	$205 \pm 2.1 < E < 235.7 \pm 204$

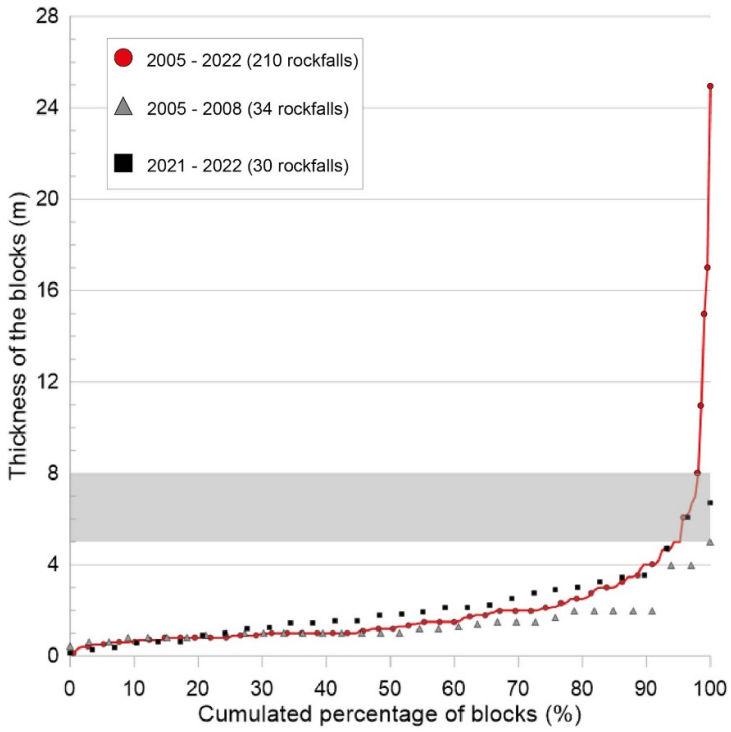

Figure 5. Maximum detachment depth from the 2005–2022 inventory. Red dots are for the entire 2005–2022 period. Grey rectangle: estimated depth of the active layer on the east face of Tour Ronde (see text). Grey triangles: 34 first rockfalls (2005–2008). Black squares: 30 last rockfalls (2021–2022).

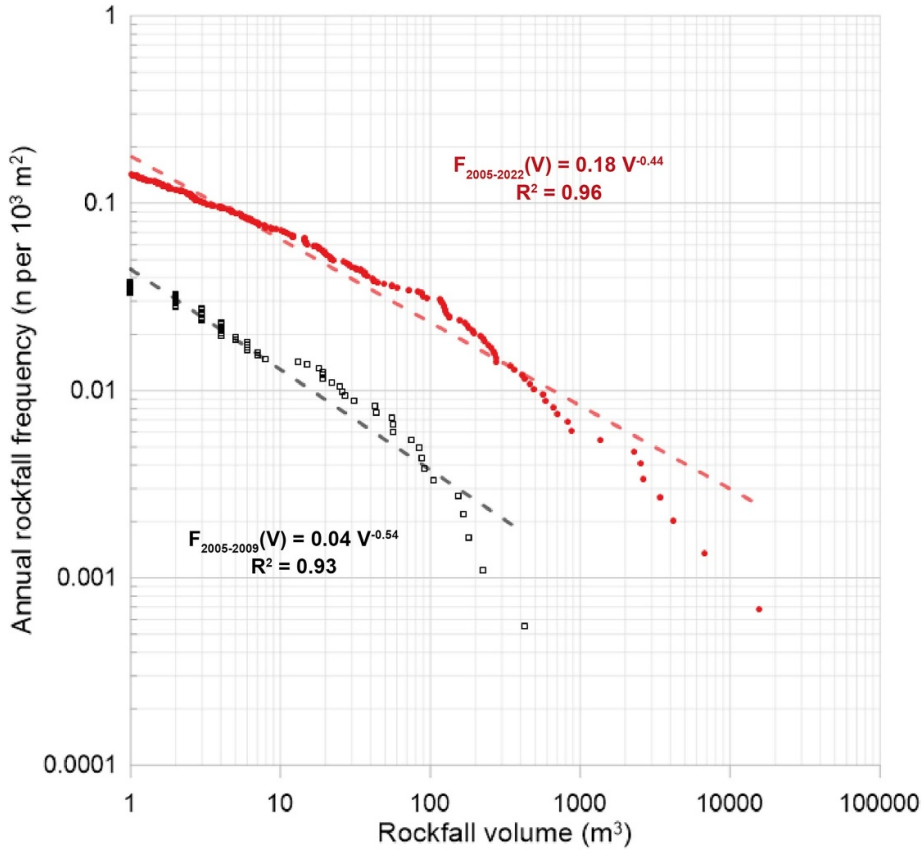

Figure 6. Magnitude-frequency distribution for all rockfalls between 2005 and 2022 (red dots). For comparison, black squares are 66 rockfalls from Ravanel *et al* (2011) in the Mont-Blanc massif, including eight rock walls located between 3320 and 4165 m (total volume: 2223 m^3).

5. Discussion

5.1. Rock wall erosion rate

In the Hohe Tauern range culminating at 3203 m (Austrian Alps), Hartmeyer *et al* (2020b) measured a mean annual erosion rate of 1.9 mm yr^{-1} over six years, with a maximum of 10.3 mm yr^{-1}. In the Hungerli valley (Swiss Alps), Draebing *et al* (2022) found a maximum erosion rate of 1.7 mm yr^{-1} over three years for rock walls at 3100–3200 m. On rock walls in the MBM, Ravanel *et al* (2011) measured erosion rates ranging from 0.03 (Piliers du Frêney, over three years) to 6.3 mm yr^{-1} (Aiguille Blanche de Peuterey, over three years). Guerin *et al* (2020) found on the west face of the Drus (2730–3730 m) an erosion rate of 14.4 mm yr^{-1} over 11 years. The mean erosion rate of 18.3 ± 0.2 mm yr^{-1} at TREF is thus the highest measured in the European Alps.

Rabatel *et al* (2008) found an erosion rate of 8.4 mm yr^{-1} at TREF between 2005 and 2006. The 2021–2022 erosion rate is now almost six times higher (47.6 ± 6.1 mm yr^{-1}). During the 18 years of the scanning period, the annual erosion rate at TREF has often been higher than at other Alpine rock walls, and it abruptly increased from 2015, with a minimum value of 12 mm yr^{-1} (figure 9). The mean value of annual rockfall volume has been multiplied by more than eight between 2005–2014 and 2016–2022 (500 and 4527 m^3 yr^{-1}, respectively; figure 9).

The erosion rate of 205 mm yr^{-1} in 2015 resulted from the large rockfall of August 27. This highlights the need for long-term acquisition to consider the role of large and less frequent rockfalls.

5.2. Frequencies and volumes

The power law exponent *b* obtained for the overall period at TREF is 0.44 ± 0.03, slightly under most of those previously published. The most complete compilation of power laws on 32 rock walls shows a median value of the *b* exponent of 0.8 (Graber and Santi 2022). Hartmeyer *et al* (2020b) found a *b*-value of 0.64 in the Hohe Tauern range, and Draebing *et al* (2022) *b*-values ranging from 0.57 to 0.76 in the Hungerly valley. In the MBM, the *b*-value has been estimated as 0.77 ± 0.04 (Ravanel *et al* 2017) but this inventory is not exhaustive as the methods used (Ravanel and Deline 2013) under-represent volumes <300 m^3, and possibly volumes >12 × 10^3 m^3 due to the short study period. The *b*-value of Guerin *et al* (2020) and TREF, based on the same methodology, are consistent (0.48 ± 0.03 and 0.44 ± 0.03, respectively).

Since a greater the *b*-value corresponds to a greater relative contribution of small rockfalls,

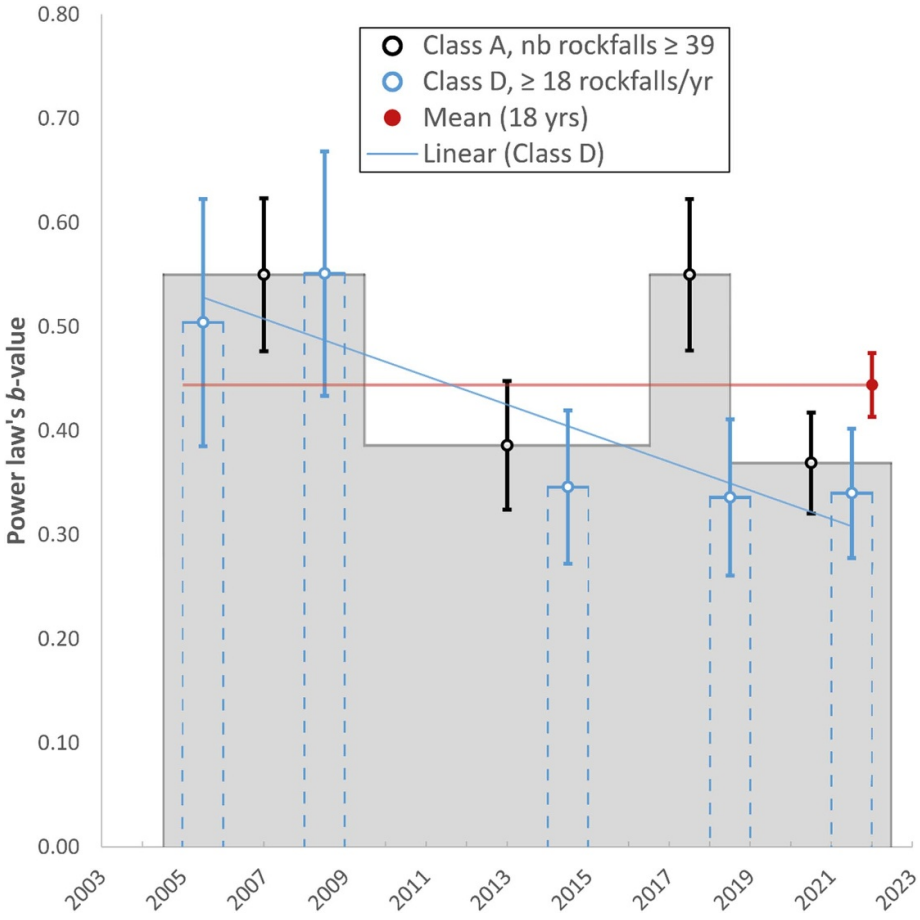

Figure 7. Power law's *b*-value depending on various binning groups. Black circles: class A. Blue circles: class D. Red dot: mean *b* for the overall period. Vertical lines: uncertainty. Grey boxes and dashed blue lines: period encompassed by the binning group.

a *b*-value of 0.4–0.5 means that the relative contribution of large rockfalls for these rock walls is greater than on other studied rock walls in the European Alps, at least for rockfalls $<10\,000$ m^3.

At TREF, the *b*-values show a weak decreasing trend (figure 7), which could illustrate the increased proportion of large rockfalls in the overall inventory that could be related to deeper rock detachment: the mean thickness increased from 1.5 to 2.1 from 2005–2008–2021–2022 (figure 2(b)). It would be tempting to link this increase to a deepening of the active layer due to the climate warming, but the following detailed analysis shows that processes are more complex.

5.3. Preconditioning factors

Review on rock slope stability (McColl 2012, Hantz *et al* 2021) argued that the structure of the rock walls (pre-existing tectonic joints, foliation, degree of fracturing) is of critical importance. The *b*-value reflects processes which are scale-invariant and possibly the rock mass structure (Turcotte 1986). The MBM granite is a very hard rock with continuous and regular brittle fractures that separate blocks generally several tens of meters wide. This can explain the high proportion of large rockfalls, evidenced by our *b*-value (0.44 ± 0.03). Nevertheless, the downward trend of the *b*-value suggests an influence of climatic conditions (Graber and Santi 2022). In addition, the TREF rockfalls occurred both in the weakly fractured Bernezat Spur and in more fractured areas, suggesting that the climatic factor could sometimes override the geology.

When shrinking, glaciers and IAs free boulders and rock masses become unstable (Krautblatter *et al* 2013). Ravanel *et al* (2023) found that after the 2003 and 2015 summer heatwaves, rockfall deposits heavily accumulated at the foot of recently deglaciated areas in the MBM due to retreat of IAs. Permafrost degradation at TREF was enhanced by the reduction of the IA surface area. Eleven rockfalls occurred in this area, accounting for 17% of the total volume during 2005–2022. In detail, 27%, 70%, 9% and 93% of the total rockfall volume detached from the upper deglaciated area in 2007–2008, 2016–2018, 2018–2019 and 2019–2021, respectively.

Glacial debuttressing is a significant preconditioning factor (Grämiger *et al* 2017, 2018): the lowering of the glacier surface induces a removal of the ice load and consequently a stress-release at the base of the rock wall (Ballantyne 2002, Cossart *et al* 2008). This debuttressing may lead to failure along critically stressed discontinuities (Davies *et al* 2001). In

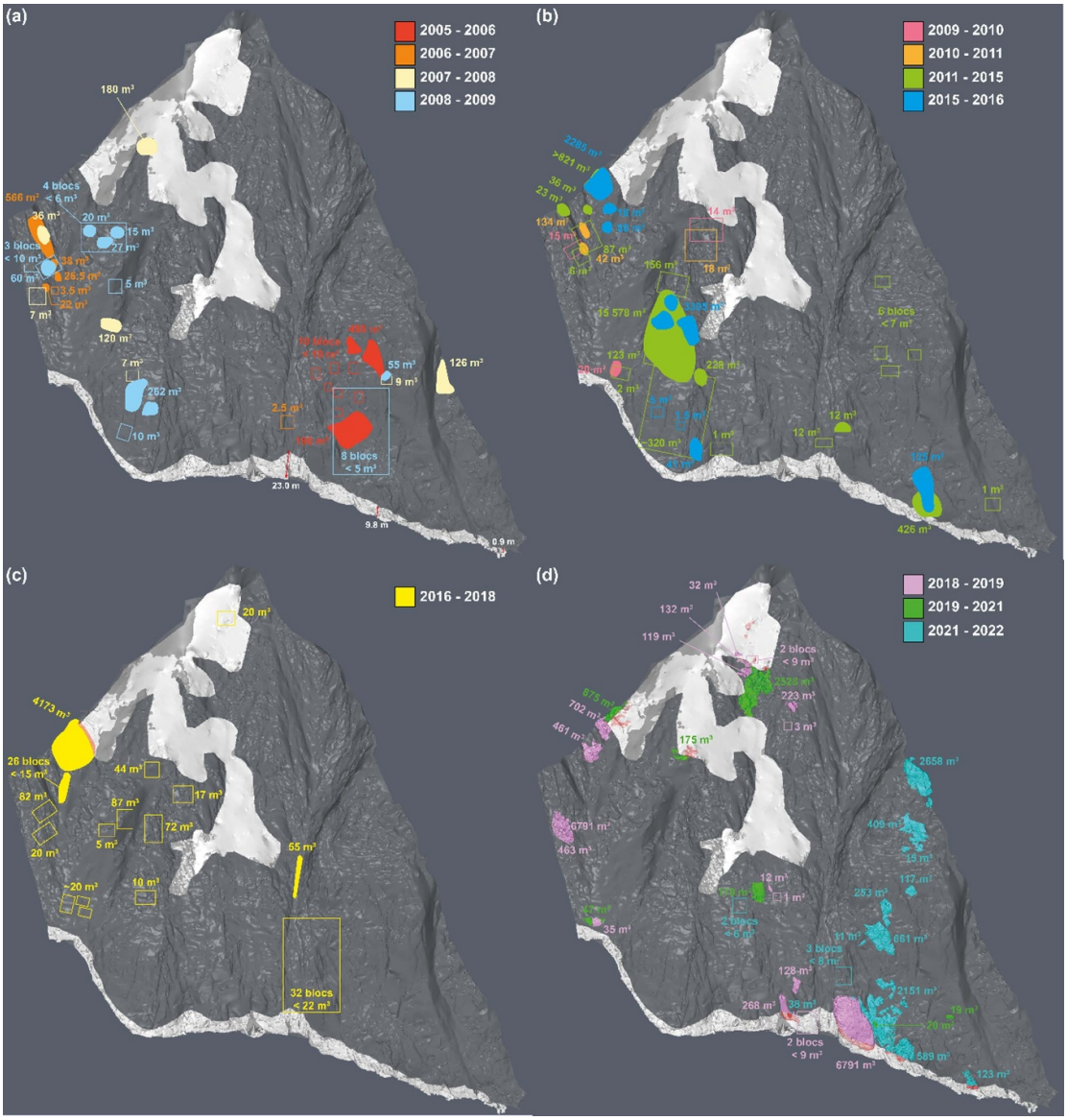

Figure 8. Rockfall distribution between 2005 and 2022 (figure 7 class A binning group). (a) From 2005 to 2009; (b) from 2009 to 2016; (c) from 2016 to 2018; (d) from 2018 to 2022. Upper white surface: ice apron extent in 2006; lower white surface: lowering of the Glacier du Géant surface between 2006 and 2022.

the MBM, glacial debuttressing could have played a role at the foot of the north side of the Aiguilles de Chamonix (Ravanel and Deline 2011) and for 15% of the rockfalls during the heat waves of 2003 and 2015 (Ravanel *et al* 2017). At TREF, rockfalls have occurred in the Glacier du Géant deglaciated area since 2006, with a delay: no rockfall occurred between 2005 and 2018, against ten between 2018 and 2022, representing 37% of the total volume of the period. Glacier retreat also exposes steep rock walls to thermal stress linked with freeze-thaw cycles. The rock surface is no longer insulated by snow and ice, and its temperature can rise further when exposed to the sun (Matsuoka and Murton 2008).

5.4. Triggering factors

The seismic activity in the vicinity of Tour Ronde east face between 2005 and 2022 is far from negligible but the intensity did not exceed IV on the European Macroseismic Scale (EMS-98) at the surface and caused no damage (Bureau Central Sismologique Français 2023), thus having minimal impact on the rock wall.

Extreme meteorological conditions with high temperature amplitudes and sudden temperature changes may result in rock wall instability in high-Alpine rock walls (Hall 1999, Matsuoka and Murton 2008, Draebing and Krautblatter 2019) that are unexpected in their location, magnitude, frequency, and timing. The year 2022 has been extremely hot in the Western Alps, particularly at high elevation. During the winter and spring, Chamonix experienced a rainfall shortage of 136 mm, while May was the warmest month since 1900 (3.5 °C above the average) and the driest since 1959. In mid-June, while the snow cover was very low, the earliest recorded heat wave started

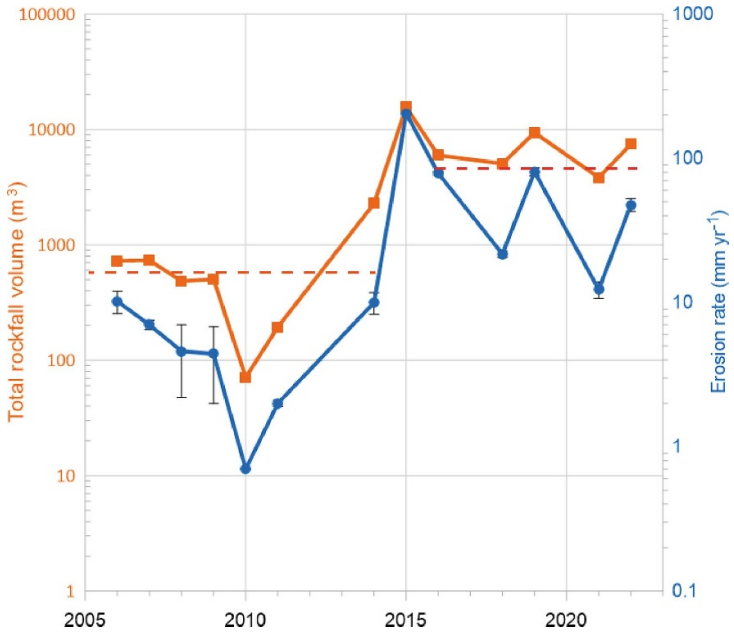

Figure 9. Evolution of the total rockfall volume (m^3) and the erosion rates (mm yr^{-1}) throughout the monitoring period (2005–2022). Note that the scan surface varied from one year to the other and the two curves are not homothetic. Dotted lines: mean annual cumulated rockfall volume for 2005–2014 and 2016–2022.

with air temperatures reaching 10.4 °C at 4750 m (Blard and Agenzia Regionale Protezione Ambiente Valle d'Aosta 2022). From July, access to mountain huts and famous Alpine summits became more difficult or even too risky. On August 24, the Fourche hut (3674 m) 1.5 km West from the TREF collapsed. The year 2022 has been exceptional but followed the trend of the summers since 2015, with hot—even scorching—summers having become the norm. Their influence is clearly recorded in the abrupt increase of the TREF rockfall occurrence since 2015.

As observed in several detachment scars, fractures in permafrost-affected rock walls are likely to contain ice and experience strong changes during warming and thaw, while freeze/thaw cycles in the active layer weaken the fractures. This can be a preparatory and sometimes triggering factor to the rockfall occurrence (Gruber and Haeberli 2007). Legay *et al* (2021) and Ravanel *et al* (2023) concluded that shallow rockfall sources (<4–6 m depth) would result from daily and seasonal freeze/thaw cycles within the active layer, whereas active layer thickening due to permafrost degradation would involve deeper source areas. The increase in the mean rockfall thickness from 1.5 to 2.1 m at TREF suggests a response to the 1 °C increase of the mean annual air temperature (MAAT) from 2006–2008–2021–2022. Between 2005 and 2014, the mean summer air temperature Chamonix was 16.2 °C, well above the MAAT of 7.9 °C. Between 2016 and 2022, these means rise to 17.6 °C and 8.8 °C, respectively (figure 10).

The depth of 95% of TREF rockfalls is <5 m, *i.e.* in the active layer. They could be linked with daily surface temperature changes, or seasonal freeze-thaw cycles (Magnin *et al* 2023). 3% of the TREF rockfalls detached below 5 and 10 m. Permafrost degradation linked to the active layer thickening could be their triggering factor (Legay *et al* 2021, Ravanel *et al* 2023), as these deep scars generally contain ice. Finally, 2% of the rockfalls are >10 m thick, *i.e.* much more than the estimation of the active layer depth.

The largest rockfall (27 August 2015) occurred during a heat wave. Modeling gives a temperature of 0 °C at a depth of 8 m (Legay *et al* 2021), much shallower than the 17 m-thick collapsed rock mass. This difference suggests (i) an entrainment effect: a large proportion of the blocks of varied thickness that form the slab were in the active layer, or (ii) water percolation in the source area, resulting in heat advection (Hasler *et al* 2011, Magnin and Josnin 2021). The second largest rockfall at TREF (4 December 2018) occurred at the winter's onset. A first motion occurred between 2017 and 2018, with 80 cm thick ice in the source area. Thermal and mechanical ice changes acted as a preconditioning factor, whereas the deep penetration of heat during the summer and autumn would have triggered the rockfall (Magnin *et al* 2015b).

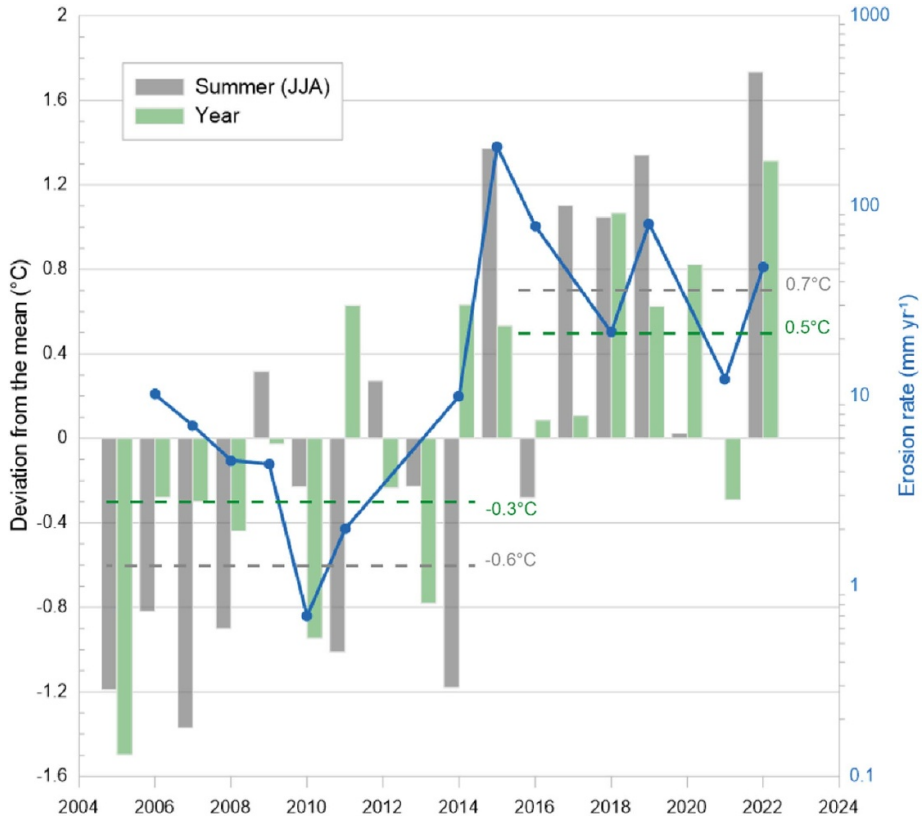

Figure 10. Deviation from the mean annual and summer air temperatures in Chamonix (1042 m) and erosion rates throughout the monitoring period (2005–2022). JJA: June-July-August. Dotted lines: mean deviation from the mean annual and summer air temperatures for 2005–2014 and 2016–2022.

6. Conclusions

A 18 year rockfall inventory (2005–2022) of the east face of Tour Ronde (3440–3792 m), based on 15 TLS acquisitions, provides unprecedented insights into rockfall dynamics in deglaciating and warming permafrost-affected rock walls. The main results of the analysis of this inventory are:

- The mean annual rock wall erosion rate of 18.3 mm yr^{-1} at TREF between 2005 and 2022 is much higher than comparable rates from European Alps. Two distinct periods are evidenced, with a mean annual rockfall volume of 500 m^3 yr^{-1} for 2005–2014 and 4527 m^3 yr^{-1} for 2016–2022.
- The rockfall magnitude-frequency relationship follows a power law with a *b*-value of 0.44 $\pm$ 0.03, which has decreased from 0.55 $\pm$ 0.07 in 2005–2009 to 0.37 $\pm$ 0.05 in 2019–2022. This decrease could be linked with the increase of the relative contribution of large rockfalls since 2005.
- The glacier shrinkage at the foot of the rock wall favored rockfall activity: 75% of the total volume for 2018–2019 and 32% for 2021–2022 detached from areas freed up by a lowering of around 10 m of the glacier surface elevation during the last 15 years. The ice apron surface area, reduced by two-thirds since 2006, also increased the rockfall occurrence with 9% and 93% of the period rockfall volume originated from the upper deglaciated area for 2018–2019 and 2019–2021, respectively.
- Ninety five percent of the rockfalls are <5 m thick. Thermal modeling suggests that most of the rock mass was located in the active layer before collapsing, which implies a dominant role for freeze/thaw cycles. The increase of annual rockfall volume since 2015 suggests that summer heatwaves have more influence than the increase in the average annual temperature (0.5 °C 10 yr^{-1} in Chamonix).

The increase in rockfall activity and erosion rate highlights a climatic driver. This has a significant impact on mountaineering. Such impact will likely increase with the predicted increase in heatwave duration and frequency (IPCC 2018), while high-elevated tourist infrastructure like huts and cable-cars in the European Alps may be threatened. Therefore, the TREF dataset could serve as a basis for modeling rockfall dynamics in high mountain regions for the next decades including various climatic scenarios. To support such modeling, more work needs to be done on the rock wall fracturing analysis to study the influence of fractures types and distribution on block stability. Similarly, continuous temperature data extending

over a longer period would be beneficial for a better understanding of the processes.

Data availability statement

All data that support the findings of this study are included within the article (and any supplementary files).

Acknowledgments

This study received financial support from the projects 'EU ALCOTRA PERMAdataROC', 'EU AlpineSPACE PermaNet', 'EU ALCOTRA PrévRisk Haute Montagne', 'EU ALCOTRA AdaPT Mont-Blanc', and 'EU ALCOTRA PrévRisk CC'. The authors thank C.M.B.H (Chamonix Mont-Blanc Hélicoptères), the ENSA (École Nationale de Ski et d'Alpinisme), Stéphane Jaillet for helping out in the field, and Paolo Pogliotti from the ARPA (Agenzia Regionale Protezione Ambiente Valle d'Aosta) for sharing temperature data recorded on the Italian side of the Mont-Blanc. Two anonymous reviewers are acknowledged for their comments that helped to improve the manuscript.

References

Aki K 1965 Maximum likelihood estimate of b in the formula log N = a-bM *Bull. Earthq. Res. Inst.* **43** 237–9

Ballantyne C K 2002 Paraglacial geomorphology *Quat. Sci. Rev.* **21** 1935–2017

Bertini G, Marcucci M, Nevini R, Passerini P and Sguazzoni G 1985 Patterns of faulting in the Mont Blanc granite *Tectonophysics* **111** 65–106

Biskaborn B K *et al* 2019 Permafrost is warming at a global scale *Nat. Commun.* **10** 264

Blard P H (Agenzia Regionale Protezione Ambiente Valle d'Aosta (ARPA VdA)) 2022 Twitter (available at: https://twitter.com/BlardPh/status/1538188788748496898)

Bommer C, Phillips M and Arenson L U 2010 Practical recommendations for planning, constructing and maintaining infrastructure in mountain permafrost: mountain infrastructure *Permaf. Periglac. Process* **21** 97–104

Bureau Central Sismologique Français (BCSF) 2023 France Séisme French (available at: www.franceseisme.fr/donnees/intensites/carte.php) (Accessed December 2023)

Bussy F and von Raumer J 1994 U-Pb geochronology of Palaeozoic magmatic events in the Mont-Blanc Crystalline Massif, Western Alps *Swiss Bull. Mineral. Petrol.* **74** 514–5

Cara M, Schlupp A and Sira C 2007. Observations sismologiques: sismicité de la France en 2003, 2004 et 2005 (in French) (Bureau central sismologique français. ULP/EOST—CNRS/INSU)

Chiarle M, Geertsema M, Mortara G and Clague J J 2021 Relations between climate change and mass movement: perspectives from the Canadian Cordillera and the European Alps *Glob. Planet. Change* **202** 1–25

Cossart E, Braucher R, Fort M, Bourlès D L and Carcaillet J 2008 Slope instability in relation to glacial debuttressing in alpine areas (Upper Durance catchment, southeastern France): evidence from field data and 10Be cosmic ray exposure ages *Geomorphology* **95** 3–26

Curtaz M, Ferrero A M, Roncella R, Segalini A and Umili G 2014 Terrestrial photogrammetry and numerical modelling for the stability analysis of rock slopes in high mountain areas: aiguilles marbrées case *Rock Mech. Rock Eng.* **47** 605–20

Davies M C R, Hamza O and Harris C 2001 The effect of rise in mean annual temperature on the stability of rock slopes containing ice-filled discontinuities *Permaf. Periglac. Process* **12** 137–44

Deline P 2001 Recent Brenva rock avalanches (valley of Aosta): new chapter in an old story? *Geogr. Fis. Din. Quat.* **5** 55–63

Deline P, Akçar N, Ivy-Ochs S and Kubik P W 2015 Repeated Holocene rock avalanches onto the Brenva glacier, Mont Blanc massif, Italy: a chronology *Quat. Sci. Rev.* **126** 186–200

Deline P, Gardent M, Magnin F and Ravanel L 2012 The morphodynamics of the Mont Blanc massif in a changing cryosphere: a comprehensive review *Geogr. Ann.* A **94** 265–83

Deline P and Kirkbride M P 2009 Rock avalanches on a glacier and morainic complex in Haut Val Ferret (Mont Blanc Massif, Italy) *Geomorphology* **103** 80–92

Draebing D and Krautblatter M 2019 The efficacy of frost weathering processes in alpine rockwalls *Geophys. Res. Lett.* **46** 6516–24

Draebing D, Krautblatter M and Dikau R 2014 Interaction of thermal and mechanical processes in steep permafrost rock walls: a conceptual approach *Geomorphology* **226** 226–35

Draebing D, Mayer T, Jacobs B and McColl S T 2022 Alpine rockwall erosion patterns follow elevation-dependent climate trajectories *Commun. Earth Environ.* **3** 1–12

Dussauge C, Grasso J-R and Helmstetter A 2003 Statistical analysis of rockfall volume distributions: implications for rockfall dynamics *J. Geophys. Res.* **108** 1–11

Duvillard P-A, Ravanel L, Marcer M and Schoeneich P 2019 Recent evolution of damage to infrastructure on permafrost in the French Alps *Reg. Environ. Change* **19** 1281–93

Duvillard P-A, Ravanel L, Schoeneich P, Deline P, Marcer M and Magnin F 2021 Qualitative risk assessment and strategies for infrastructure on permafrost in the French Alps *Cold Reg. Sci. Technol.* **189** 103311

Fischer M, Huss M and Hoelzle M 2015 Surface elevation and mass changes of all Swiss glaciers 1980–2010 *Cryosphere* **9** 525–40

Frauenfelder R, Isaksen K, Lato M J and Noetzli J 2018 Ground thermal and geomechanical conditions in a permafrost-affected high-latitude rock avalanche site (Polvartinden, northern Norway) *Cryosphere* **12** 1531–50

Gardent M, Rabatel A, Dedieu J-P and Deline P 2014 Multitemporal glacier inventory of the French Alps from the late 1960s to the late 2000s *Glob. Planet. Change* **120** 24–37

Girardeau-Montaut D 2015 CloudCompare (GPL software, EDF RandD, Telecom ParisTech)

Gischig V S, Moore J R, Evans K F, Amann F and Loew S 2011 Thermomechanical forcing of deep rock slope deformation: 1. Conceptual study of a simplified slope *J. Geophys. Res.* **116** F04010

Graber A and Santi P 2022 Power law models for rockfall frequency-magnitude distributions: review and identification of factors that influence the scaling exponent *Geomorphology* **418** 1–23

Grämiger L M, Moore J R, Gischig V S, Ivy-ochs S and Loew S 2017 Beyond debuttressing: mechanics of paraglacial rock slope damage during repeat glacial cycles *J. Geophys. Res.* **122** 1004–36

Grämiger L M, Moore J R, Gischig V S and Loew S 2018 Thermomechanical stresses drive damage of alpine valley rock walls during repeat glacial cycles *J. Geophys. Res.* **123** 2620–46

Gruber S and Haeberli W 2007 Permafrost in steep bedrock slopes and its temperature-related destabilization following climate change *J. Geophys. Res.* **112** 1–10

Gruber S, Hoelzle M and Haeberli W 2004 Permafrost thaw and destabilization of Alpine rock walls in the hot summer of 2003 *Geophys. Res. Lett.* **31** 1–4

Guerin A, Ravanel L, Matasci B, Jaboyedoff M and Deline P 2020 The three-stage rock failure dynamics of the Drus (Mont Blanc massif, France) since the June 2005 large event *Sci. Rep.* **10** 1–20

Guillet G and Ravanel L 2020 Variations in surface area of six ice aprons in the Mont-Blanc massif since the little ice age *J. Glaciol.* **66** 777–89

Haeberli W, Huggel C, Kääb A, Zgraggen-Oswald S, Polkvoj A, Galushkin I, Zotikov I and Osokin N 2004 The Kolka-Karmadon rock/ice slide of 20 September 2002: an extraordinary event of historical dimensions in North Ossetia, Russian Caucasus *J. Glaciol.* **50** 533–46

Hall K 1999 The role of thermal stress fatigue in the breakdown of rock in cold regions *Geomorphology* **31** 47–63

Hantz D, Corominas J, Crosta G B and Jaboyedoff M 2021 Definitions and concepts for quantitative rockfall hazard and risk analysis *Geosciences* **11** 158

Hantz D, Dussauge-Peisser C, Jeannin M and Vengeon J-M 2003 Rock fall hazard assessment: from qualitative to quantitative failure probability *Int. Conf. on Fast Slope Movements, Prediction and Prevention for Risk Mitigation* (*Naples,* 2003) pp 263–7

Hartmeyer I, Delleske R, Keuschnig M, Krautblatter M, Lang A, Schrott L and Otto J-C 2020a Current glacier recession causes significant rockfall increase: the immediate paraglacial response of deglaciating cirque walls *Earth Surf. Dyn.* **8** 729–51

Hartmeyer I, Keuschnig M, Delleske R, Krautblatter M, Lang A, Schrott L, Prasicek G and Otto J-C 2020b A 6-year lidar survey reveals enhanced rockwall retreat and modified rockfall magnitudes/frequencies in deglaciating cirques *Earth Surf. Dyn.* **8** 753–68

Hasler A, Gruber S, Font M and Dubois A 2011 Advective heat transport in frozen rock clefts: conceptual model, laboratory experiments and numerical simulation *Permafr. Periglac.* **22** 378–89

Huggel C 2009 Recent extreme slope failures in glacial environments: effects of thermal perturbation *Quat. Sci. Rev.* **28** 1119–30

Huggel C, Allen S, Deline P, Fischer L, Noetzli J and Ravanel L 2012 Ice thawing, mountains falling-are alpine rock slope failures increasing? *Geol. Today* **28** 98–104

Huggel C, Zgraggen-Oswald S, Haeberli W, Kääb A, Polkvoj A, Galushkin I and Evans S G 2005 The 2002 rock/ice avalanche at Kolka/Karmadon, Russian Caucasus: assessment of extraordinary avalanche formation and mobility, and application of QuickBird satellite imagery *Nat. Hazards Earth Syst. Sci.* **5** 173–87

IPCC, 2018. Global warming of 1.5 °C: IPCC special report on impacts of global warming of 1.5 °C above pre-industrial levels in context of strengthening response to climate change, sustainable development, and efforts to eradicate poverty (Cambridge University Press) (available at: www.ipcc.ch/sr15/)

Jibson R W, Harp E L, Schulz W and Keefer D K 2006 Large rock avalanches triggered by the M 7.9 denali fault, Alaska, earthquake of 3 November 2002 *Eng. Geo.* **83** 144–60

Kargel J S *et al* 2016 Geomorphic and geologic controls of geohazards induced by Nepal's 2015 Gorkha earthquake *Science* **351** 140

Kaushik S, Ravanel L, Magnin F, Trouvé E and Yan Y 2022 Ice aprons in the Mont Blanc massif (Western European Alps): topographic characteristics and relations with glaciers and other types of perennial surface ice features *Remote Sens.* **14** 1–24

Kazhdan M, Chuang M, Rusinkiewicz S and Hoppe H 2020 Poisson surface reconstruction with envelope constraints *Comput. Graph. Forum* **39** 173–82

Keefer D K 2002 Investigating landslides caused by earthquakes—a historical review *Surv. Geophys.* **23** 473–510

Kenner R, Phillips M, Danioth C, Denier C, Thee P and Zgraggen A 2011 Investigation of rock and ice loss in a recently deglaciated mountain rock wall using terrestrial laser scanning: gemsstock, Swiss Alps *Cold Reg. Sci. Technol.* **67** 157–64

Krautblatter M, Funk D and Günzel F K 2013 Why permafrost rocks become unstable: a rock-ice-mechanical model in time and space *Earth Surf. Process. Landf.* **38** 876–87

Legay A, Magnin F and Ravanel L 2021 Rock temperature prior to failure: analysis of 209 rockfall events in the Mont Blanc massif (Western European Alps) *Permaf. Periglac. Process* **32** 520–36

Leica Geosystems, Hexagon 2023 Leica Cyclone 3DR

Lipovsky P S *et al* 2008 The July 2007 rock and ice avalanches at Mount Steele, St. Elias Mountains, Yukon, Canada *Landslides* **5** 445–55

Magnin F *et al* 2023 From rockwall observation to operational solutions: nearly 20 years of cryo-gravitational hazard studies in Mont-Blanc massif *J. Alpine Res.* **111** 1–19

Magnin F, Brenning A, Bodin X, Deline P and Ravanel L 2015a Statistical modelling of rock wall permafrost distribution: application to the Mont Blanc massif *Géomorphologie* **21** 145–62

Magnin F, Deline P, Ravanel L, Noetzli J and Pogliotti P 2015b Thermal characteristics of permafrost in the steep alpine rock walls of the Aiguille du Midi (Mont Blanc Massif, 3842 m a.s.l) *Cryosphere* **9** 109–21

Magnin F and Josnin J - Y 2021 Water flows in rock wall permafrost: a numerical approach coupling hydrological and thermal processes *JGR Earth Surf.* **126** 1–20

Magnin F, Josnin J-Y, Ravanel L, Pergaud J, Pohl B and Deline P 2017 Modelling rock wall permafrost degradation in the Mont Blanc massif from the LIA to the end of the 21st century *Cryosphere* **11** 1813–34

Matasci B, Stock G M, Jaboyedoff M, Carrea D, Collins B D, Guérin A, Matasci G and Ravanel L 2018 Assessing rockfall susceptibility in steep and overhanging slopes using three-dimensional analysis of failure mechanisms *Landslides* **15** 859–78

Matsuoka N and Murton J 2008 Frost weathering: recent advances and future directions *Permaf. Periglac. Process* **19** 195–210

McColl S T 2012 Paraglacial rock-slope stability *Geomorphology* **153–154** 1–16

Mergili M, Jaboyedoff M, Pullarello J and Pudasaini S P 2020 Back calculation of the 2017 Piz Cengalo–Bondo landslide cascade with r.avaflow: what we can do and what we can learn *Nat. Hazards Earth Syst. Sci.* **20** 505–20

Mourey J, Moret O, Descamps P and Bozon S, 2018 Accidentology of the normal route up Mont Blanc between 1990 and 2017 (Fondation Petzl)

Mourey J, Ravanel L, Lambiel C, Strecker J and Piccardi M 2019 Access routes to high mountain huts facing climate-induced environmental changes and adaptive strategies in the Western Alps since the 1990s *Nor. Geogr. Tidsskr.—Norw. J. Geogr.* **73** 215–28

Noetzli J, Hoelzle M and Haeberli W 2003 Mountain permafrost and recent Alpine rock-fall events: a GIS-based approach to determine critical factors *8th Int. Conf. on Permafrost* (*Zürich, Switzerland*) pp 827–32

Oppikofer T, Jaboyedoff M, Blikra L, Derron M-H and Metzger R 2009 Characterization and monitoring of the Åknes rockslide using terrestrial laser scanning *Nat. Hazards Earth Syst. Sci.* **9** 1003–19

Phillips M, Wolter A, Lüthi R, Amann F, Kenner R and Bühler Y 2017 Rock slope failure in a recently deglaciated permafrost rock wall at Piz Kesch (Eastern Swiss Alps), February 2014: rock slope failure in a permafrost rock wall at Piz Kesch, Swiss alps *Earth Surf. Process. Landf.* **42** 426–38

Pirulli M 2009 The Thurwieser rock avalanche (Italian Alps): description and dynamic analysis *Eng. Geol.* **109** 80–92

Rabatel A, Deline P, Jaillet S and Ravanel L 2008 Rock falls in high-alpine rock walls quantified by terrestrial lidar measurements: a case study in the Mont Blanc area *Geophys. Res. Lett.* **35** 1–5

Ravanel L, Allignol F, Deline P, Gruber S and Ravello M 2010 Rock falls in the Mont Blanc Massif in 2007 and 2008 *Landslides* **7** 493–501

Ravanel L, Bodin X and Deline P 2014 Using terrestrial laser scanning for the recognition and promotion of high-alpine geomorphosites *Geoheritage* **6** 129–40

Ravanel L and Deline P 2008 The west face of les drus (Mont-Blanc massif): slope instability in a high-Alpine steep rock wall since the end of the little ice age *Géomorphologie* **14** 261–72

Ravanel L and Deline P 2011 Climate influence on rockfalls in high-Alpine steep rockwalls: the north side of the Aiguilles de Chamonix (Mont Blanc massif) since the end of the 'little ice age *Holocene* **21** 357–65

Ravanel L and Deline P 2013 A network of observers in the Mont-Blanc massif to study rockfall from high Alpine rockwalls *Geogr. Fis. Din. Quat.* **36** 151–8

Ravanel L, Deline P and Jaillet S 2011 Four years of monitoring of rockwall morphodynamics in the Mont-Blanc massif by terrestrial laser scanning *Collection EDYTEM* **12** 69–76

Ravanel L, Guillet G, Kaushik S, Preunkert S, Malet E, Magnin F, Trouvé E, Montagnat M, Yan Y and Deline P 2023 Ice aprons on steep high-alpine slopes: insights from the Mont-Blanc massif, Western Alps *J. Glaciol.* **69** 1275–91

Ravanel L, Magnin F and Deline P 2017 Impacts of the 2003 and 2015 summer heatwaves on permafrost-affected rock-walls in the Mont Blanc massif *Sci. Total Environ.* **609** 132–43

RGI Consortium, 2017. Randolph glacier inventory—a dataset of global glacier outlines

Rosser N J, Petley D N, Lim M, Dunning S A and Allison R J 2005 Terrestrial laser scanning for monitoring the process of hard rock coastal cliff erosion *Q. J. Eng. Geol. Hydrogeol.* **38** 363–75

Rossi M, 2005. Déformation, transferts de matière et de fluide dans la croûte continentale: application aux massifs cristallins externes des Alpes *Géologie appliquée* (Université Joseph-Fourier, Grenoble I) (in French)

Schiermeier Q 2003 Alpine thaw breaks ice over permafrost's role *Nature* **424** 712

Soulé B, Lefèvre B, Boutroy E, Reynier V, Roux F and Corneloup J 2014 *Accidentology of Mountain Sports* vol 1 (Petzl Foundation) pp 1–48

Stoffel M and Huggel C 2012 Effects of climate change on mass movements in mountain environments *Prog. Phys. Geogr.* **36** 421–39

Turcotte D L 1986 Fractals and fragmentation *J. Geophys. Res.* **91** 1921–6

Vincent C, Fischer A, Mayer C, Bauder A, Galos S P, Funk M, Thibert E, Six D, Braun L and Huss M 2017 Common climatic signal from glaciers in the European Alps over the last 50 years *Geophys. Res. Lett.* **44** 1376–83

Walter F *et al* 2020 Direct observations of a three million cubic meter rock-slope collapse with almost immediate initiation of ensuing debris flows *Geomorphology* **351** 106933